

## Microporous Metal–Organic Framework Constructed from Heptanuclear Zinc Carboxylate Secondary Building Units

Qian-Rong Fang,<sup>[a]</sup> Guang-Shan Zhu,<sup>\*[a]</sup> Ming Xue,<sup>[a]</sup> Qing-Lin Zhang,<sup>[c]</sup> Jin-Yu Sun,<sup>[a]</sup> Xiao-Dan Guo,<sup>[a]</sup> Shi-Lun Qiu,<sup>\*[a]</sup> Shi-Tao Xu,<sup>[b]</sup> Ping Wang,<sup>[b]</sup> De-Jun Wang,<sup>[c]</sup> and Yen Wei<sup>[d]</sup>

**Abstract:** A novel, three-dimensional, noninterpenetrating microporous metal–organic framework (MOF),  $[\text{Zn}_7\text{O}_2(\text{pda})_5(\text{H}_2\text{O})_2] \cdot 5\text{DMF} \cdot 4\text{EtOH} \cdot 6\text{H}_2\text{O}$  (**1**) ( $\text{H}_2\text{PDA} = p$ -phenylenediacrylic acid, DMF = *N,N*-dimethylformamide, EtOH = ethanol), was synthesized by constructing heptanuclear zinc carboxylate secondary building units (SBUs) and by using rigid and linear aromatic carboxylate ligands, PDA. The X-ray crystallographic data reveals that the seven zinc centers of **1** are held together with ten carboxylate groups of the PDA ligands and four

water molecules to form a heptametallic SBU,  $\text{Zn}_7\text{O}_4(\text{CO}_2)_{10}$ , with dimensions of  $9.8 \times 9.8 \times 13.8 \text{ \AA}^3$ . Furthermore, the heptametallic SBUs are interconnected by PDA acting as linkers, thereby generating an extended network with a three-dimensional, noninterpenetrating, intersecting large-channel

system with spacing of about  $17.3 \text{ \AA}$ . As a microporous framework, polymer **1** shows adsorption behavior that is favorable towards  $\text{H}_2\text{O}$  and  $\text{CH}_3\text{OH}$ , and substantial  $\text{H}_2$  uptake. In terms of the heptanuclear zinc carboxylate SBUs, polymer **1** exhibits interesting photoelectronic properties, which would facilitate the exploration of new types of semiconducting materials, especially among MOFs containing multinuclear metal carboxylate SBUs.

**Keywords:** hydrogen storage • metal–organic frameworks • microporous materials • photoelectronic properties • secondary building units

### Introduction

The synthesis and characterization of porous metal–organic frameworks (MOFs) have attracted much attention, owing to their enormous variety of interesting structural topologies

and potential applications as functional materials.<sup>[1–12]</sup> These porous MOFs are produced by utilizing polyatomic organic ligands as linkers and the well-defined coordination geometries of metal centers as nodes.<sup>[13,14]</sup> Recently, Kitagawa et al. examined the adsorption behavior of these porous MOFs towards some small molecules, such as oxygen and methane.<sup>[15]</sup> In addition, the study by Yaghi et al. suggested that such porous MOFs are able to store hydrogen at a capacity unmatched by other materials.<sup>[16]</sup> However, successful synthetic strategies are still a formidable challenge for the preparation of large, porous MOFs with promising applications, owing to a strong tendency of interpenetration in these very open architectures and the collapse of the host framework, which is caused by the evacuation of guest molecules from the pores.

As an effective and powerful synthetic strategy, the construction of clustered metal carboxylate entities as secondary building units (SBUs) has been shown to provide a new generation of highly porous MOFs.<sup>[17]</sup> To date, many MOFs constructed from zinc carboxylate SBUs have been synthesized, and usually comprise of two, three, or four zinc centers.<sup>[18–20]</sup> Interestingly, Zheng et al. described a novel

[a] Dr. Q.-R. Fang, Prof. G.-S. Zhu, Dr. M. Xue, Dr. J.-Y. Sun, Dr. X.-D. Guo, Prof. S.-L. Qiu  
State Key Laboratory of Inorganic Synthesis and Preparative Chemistry  
Jilin University, Changchun 130012 (China)  
Fax: (+86)431-516-8331  
E-mail: zhugs@mail.jlu.edu.cn  
sqiu@mail.jlu.edu.cn

[b] Dr. S.-T. Xu, Prof. P. Wang  
State Key Laboratory of RSA, Institute of Metal Research  
Chinese Academy of Sciences, Shenyang 110016 (China)

[c] Dr. Q.-L. Zhang, Prof. D.-J. Wang  
College of Chemistry, Jilin University, Changchun 130023 (China)

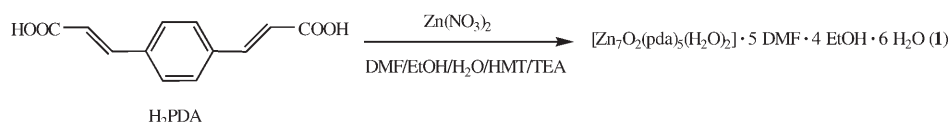
[d] Prof. Y. Wei  
Department of Chemistry, Drexel University  
Philadelphia, PA 19104 (USA)

Supporting information for this article is available on the WWW under <http://www.chemeurj.org/> or from the author.

MOF,  $[\text{Zn}_8(\text{SiO}_4)(\text{C}_8\text{H}_4\text{O}_4)_6]_n$  ( $\text{C}_8\text{H}_4\text{O}_4$ =isophthalate), with a diamondoid framework structure constructed from hexahedron-like  $\text{Zn}_8(\text{SiO}_4)$  cores and  $\text{C}_8\text{H}_4\text{O}_4$  linkers.<sup>[21]</sup> With the expansion of such zinc carboxylate SBUs, it is believed that new MOFs with extra-large pores can be synthesized. Furthermore, if the dimensions of these SBUs are expanded further, such MOFs might exhibit characteristics (such as the optoelectronic property) similar to those of nanosized metal oxide semiconducting materials.<sup>[22]</sup> To address this issue, we present here a novel, three-dimensional, noninterpenetrating MOF with an intersecting channel system,  $[\text{Zn}_7\text{O}_2(\text{pda})_5(\text{H}_2\text{O})_2] \cdot 5 \text{ DMF} \cdot 4 \text{ EtOH} \cdot 6 \text{ H}_2\text{O}$  (**1**) ( $\text{H}_2\text{PDA}$ =*p*-phenylene-diacrylic acid, DMF=*N,N*-dimethylformamide, EtOH=ethanol) with spacing of about 17.3 Å, by constructing heptanuclear zinc carboxylate SBUs and by using a rigid and linear aromatic carboxylate, PDA. The formulations of **1** were established by the results of IR spectroscopy, microanalysis, and thermogravimetric analysis (TGA). The liquid adsorption,  $\text{H}_2$  storage, and photoelectronic properties of **1** were examined. To the best of our knowledge, this is the first study of the optoelectronic properties of a heptanuclear zinc-organic framework.

## Results and Discussion

Polymer **1** was synthesized under mild conditions by using hexamethylenetetramine (HMT) as the structure-directing agent, DMF/EtOH/ $\text{H}_2\text{O}$  as the solvent, and triethylamine (TEA) as the deprotonating agent (Scheme 1). Though not



Scheme 1. The synthesis of **1**.

observed in the crystalline structure, HMT apparently plays some structure-directing role, as the control reactions in the absence of HMT did not result in the network of **1**.<sup>[23]</sup> This complex was found to be insoluble in common organic solvents, such as acetone, methanol, ethanol, dichloromethane, acetonitrile, chloroform, and DMF. The crystals were characterized by IR spectroscopy, elemental analysis, and single-crystal X-ray structural analysis.

Results of the X-ray crystallography reveal that **1** crystallizes in the tetragonal group *I4cm* (No. 108). As shown in Figure 1, the fundamental building unit of **1** contains seven zinc ions, ten crystallographically equivalent PDA ligands, and four water molecules. The seven zinc centers with three octahedral and four tetrahedral coordination geometries are held together with ten carboxylate groups of the PDA ligands through bidentate or chelating/bridging bidentate coordination forms and four water molecules (two  $\mu_4$ -O atoms and two terminal oxygen atoms), to build up a seven-nuclear

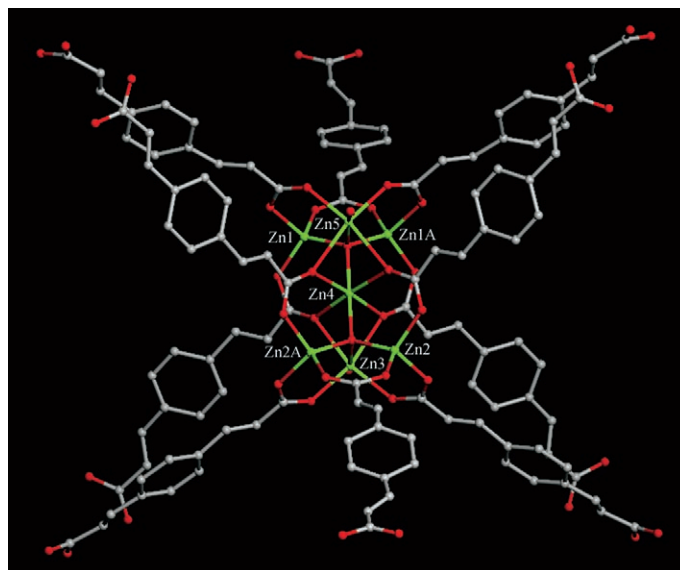


Figure 1. A view of the fundamental building unit for **1**. Color code: Zn = green; O = red; C = gray.

zinc carboxylate cluster,  $\text{Zn}_7\text{O}_4(\text{CO}_2)_{10}$  (Figure 2a,b). The dimensions of the cluster are about  $9.8 \times 9.8 \times 13.8 \text{ \AA}^3$  (measured between opposite atoms), and such multinuclear metal carboxylate clusters are very unusual in MOFs. In addition, the heptanuclear clusters, which behave as SBUs, are interconnected by PDA acting as linkers, thereby generating an extended network with a three-dimensional, noninterpenetrating, intersecting large-channel system with spacing of about 17.3 Å between the centers of adjacent clusters, as shown in Figure 2c. The interesting structural features of **1** are a single PDA molecule interconnecting adjacent SBUs along the [001] direction, and two PDA molecules linking adjacent SBUs along the [100] and [010] directions, respectively (Figure 3). In addition, the void space in **1** is filled with five DMF, four EtOH, and six  $\text{H}_2\text{O}$  guest molecules, as established by elemental analysis and TGA.<sup>[24]</sup>

To study the adsorption properties, the water and methanol adsorption isotherms for **1** were measured at room temperature (ca. 20 °C). Before recording the measurements, the sample of **1** was soaked in  $\text{CH}_2\text{Cl}_2$  for 48 h and then heated at 80 °C for 6 h to remove the included solvent molecules. As shown in Figure 4, the methanol adsorption isotherm of **1** exhibits two uptakes. Little adsorption at the outset is followed by a larger uptake that terminates in a plateau near the saturation region. This is similar to the results for some reported MOFs.<sup>[25]</sup> At saturation, the amount of methanol adsorbed by **1** is  $164.9 \text{ mg g}^{-1}$ . This is equivalent to the adsorption of about 66  $\text{CH}_3\text{OH}$  molecules per formula unit. However, type I behavior is observed for the water adsorption isotherm of **1**, which is characteristic of solids

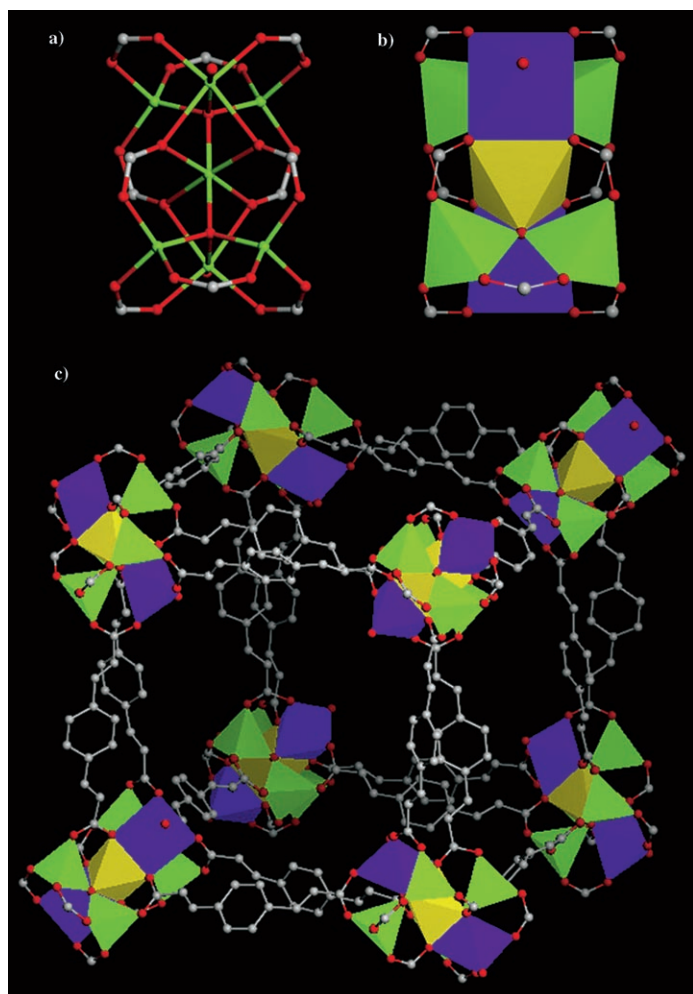


Figure 2. a) A ball and stick model of the  $\text{Zn}_7\text{O}_4(\text{CO}_2)_{10}$  SBU for **1** with dimensions of about  $9.8 \times 9.8 \times 13.8 \text{ \AA}^3$ . Color code: Zn = green; O = red; C = gray. b) The same as (a), but with the  $\text{ZnO}_4$  tetrahedra indicated in green polyhedra and the  $\text{ZnO}_6$  octahedra indicated in blue or yellow polyhedra for clarity. c) A view of the cubic cavity constructed from eight SBUs interconnected by PDA acting as linkers in **1**.

with micropores. At saturation, the amount of water adsorbed by **1** is  $166.8 \text{ mg g}^{-1}$ , which is equivalent to the adsorption of about 119  $\text{H}_2\text{O}$  molecules per formula unit. Therefore, the pore volume for **1** is estimated from the water adsorption isotherm to be approximately  $0.17 \text{ mL g}^{-1}$ .

We also examined the gas-storage behavior of **1** at room temperature. The hydrogen adsorption isotherm was recorded with the sample of **1** under different hydrogen pressures by using a conventional volumetric method (Figure 5).<sup>[26]</sup> Polymer **1** shows substantial  $\text{H}_2$  uptake that increased linearly as hydrogen pressure increased, giving 1.01 wt% at 71.43 bar, which corresponds to a  $\text{H}_2$  storage capacity of  $112.4 \text{ mL g}^{-1}$ . The  $\text{H}_2$  uptake of **1** is reversible for at least eight cycles. Even though the hydrogen uptake measured for **1** is not very high, it is comparable to  $\text{H}_2$  storage capacities of “active” carbon (CECA, France) and purified single-walled carbon nanotubes.<sup>[27]</sup> In addition, the fact that the  $\text{H}_2$

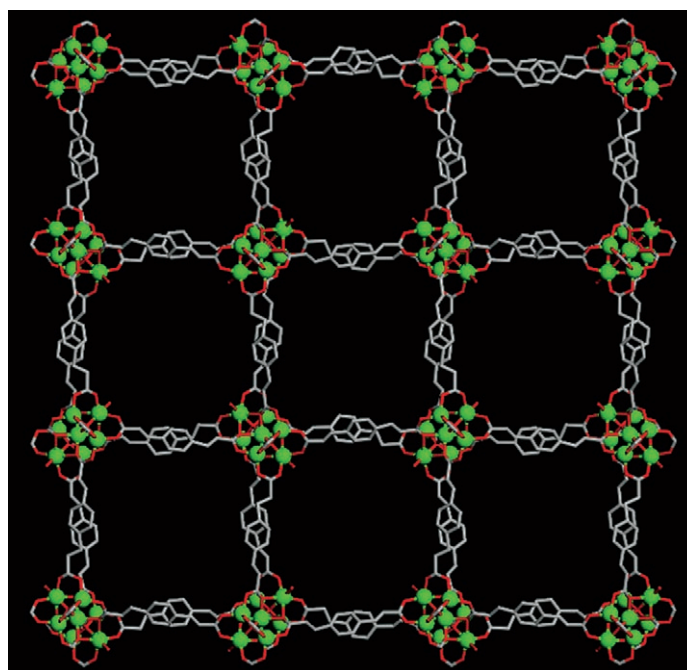


Figure 3. View along the [001] direction of **1** showing large channels with diameters of about  $17.3 \text{ \AA}$ . Color code: Zn = green (ball); O = red; C = gray.

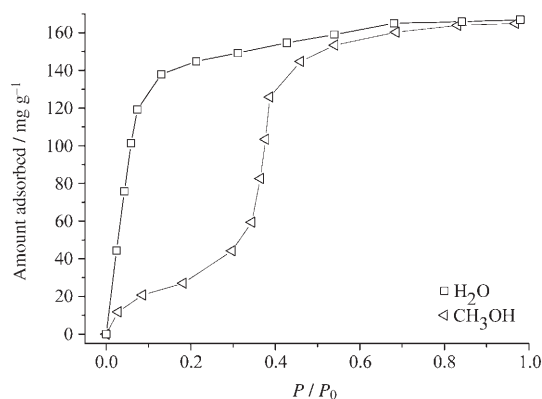


Figure 4. Water and methanol adsorption isotherms for **1** at room temperature.

storage capacity of **1** does not reach saturation at 71.43 bar indicates that this complex has yet more potential in the storage of  $\text{H}_2$ . Further research on the  $\text{H}_2$  storage is underway.

Photovoltage (PV) transients for **1** were observed under atmospheric pressure and at ambient temperature.<sup>[28]</sup> It is known that a PV signal arises upon the separation in space of light-induced excess-charge carriers, and that transient PV can be used for characterization of semiconductor materials.<sup>[29]</sup> Figure 6a shows PV transients for **1** at different intensities of the exciting laser pulse (355 nm). Clearly, the transient PV signals of **1** exhibit retardation in time, which is caused by slow and independent diffusion of excess electrons and holes. Although the intensities of the exciting

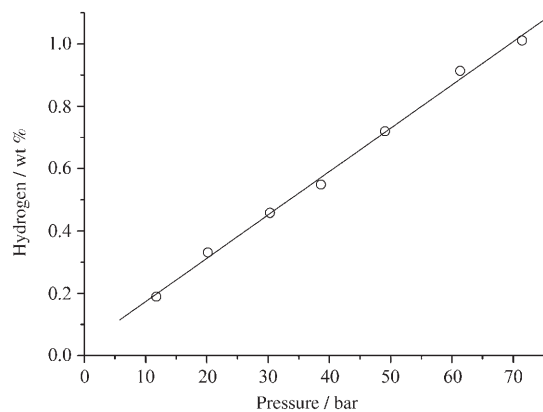


Figure 5. Hydrogen adsorption isotherm of **1** under different hydrogen pressures at room temperature.

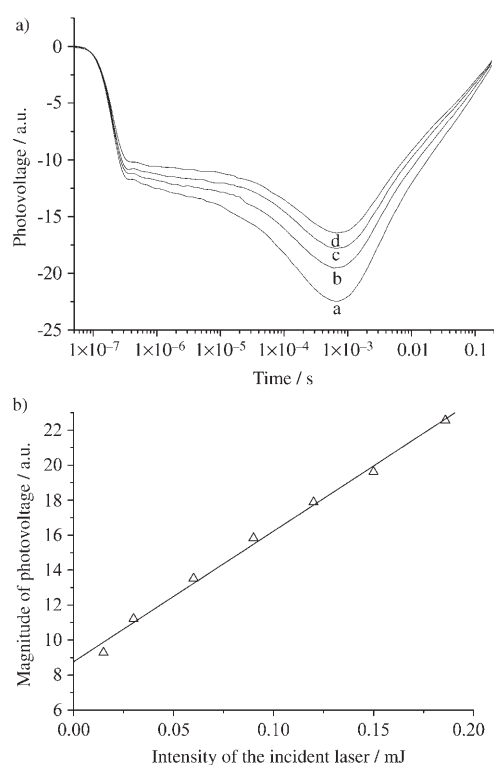


Figure 6. a) The transient photovoltage (PV) response of the ITO/polymer **1**/ITO sandwich cell under illumination of 355 nm pulse laser at various intensities. From curves a to d, the corresponding light intensities are 0.19, 0.15, 0.12, and 0.90 mJ. b) The dependence of the absolute value of the PV amplitude on the excitation intensity for the polymer **1**.

laser pulses are different (0.19, 0.15, 0.12, and 0.90 mJ), the times at which their maxima arise are similar, appearing at about  $7 \times 10^{-4}$  s. The maxima are related to the separation of charge at the polymer **1**/indium-tin oxide (ITO) interface, and the gradient of excess electron and hole concentrations is caused by nonhomogeneous absorption of light with photons of  $h\nu > E_G$ .  $E_G$  represents the optical band gap, and the diffuse reflectance UV-visible spectra for **1** gives a value of  $E_G$  close to 3.26 eV, which is similar to the reported band

gap of anatase.<sup>[30]</sup> In addition, the signals of the PV transients are negative, which suggests that the photoexcited electrons move slower than the holes towards the polymer **1**/ITO interface. The dependence of the PV signal upon the intensity of the exciting laser pulse in the maximum of the transients ( $U_{\max}^{\text{PV}}$ ) is given in Figure 6b and is linear up to 0.2 mJ. The linear dependence of  $U_{\max}^{\text{PV}}$  on intensity implies that **1** possesses the characteristic of the diffusion PV transient, but not of the Dember PV transient, which is similar to the case of nanosized metal oxide semiconductors (e.g., ZnO and TiO<sub>2</sub>).<sup>[31]</sup>

## Conclusion

By constructing heptanuclear zinc carboxylate SBUs and by using PDA ligands we have successfully synthesized a novel, three-dimensional, noninterpenetrating MOF, [Zn<sub>7</sub>O<sub>2</sub>(pda)<sub>5</sub>(H<sub>2</sub>O)<sub>2</sub>]<sub>5</sub>DMF<sub>4</sub>EtOH<sub>6</sub>H<sub>2</sub>O (**1**), with spaced, intersecting channel systems. For a microporous framework, polymer **1** shows adsorption behavior that is favorable towards H<sub>2</sub>O and CH<sub>3</sub>OH, and substantial H<sub>2</sub> uptake. More advanced research on H<sub>2</sub> storage is currently underway. In terms of heptanuclear zinc carboxylate SBUs, polymer **1** exhibits interesting photoelectronic properties, which would facilitate the exploration of new types of semiconducting materials, especially among MOFs containing multinuclear metal carboxylate SBUs.

## Experimental Section

**Materials and physical techniques:** All reagents and solvents were commercially available and were used as received without further purification. A Perkin–Elmer TGA 7 thermogravimetric analyzer was used to obtain TGA curves in air with a heating rate of 5°C min<sup>-1</sup>. Powder X-ray diffraction (XRD) data were collected by using a Siemens D5005 diffractometer with CuK<sub>α</sub> radiation ( $\lambda = 1.5418 \text{ \AA}$ ). Analyses for C, H, and N were carried out by using a Perkin–Elmer analyzer. The IR spectra were recorded (400–4000 cm<sup>-1</sup> region) by using a Nicolet Impact 410 FTIR spectrometer with KBr pellets. Liquid adsorption measurements were conducted by using a CAHN 2000 analyzer at RT. Hydrogen storage was measured with the sample under different hydrogen pressures by using a conventional volumetric method. Analyses of PV transients were conducted by having the sample in a sandwich cell (ITO/polymer **1**/ITO) and by using the light-source-monochromator-lock-in detection technique.

**Synthesis of 1:** Zn(NO<sub>3</sub>)<sub>2</sub>·6H<sub>2</sub>O (0.15 g, 0.50 mmol), PDA (0.04 g, 0.2 mmol), HMT (0.01 g, 0.1 mmol), DMF (10.0 mL), ethanol (2.0 mL), and H<sub>2</sub>O (2.0 mL) were placed in a 25 mL vial to form a solution under stirring. After stirring in air for 1 h, the vial was set in a beaker (100 mL) containing an ethanol solution (5 mL) of triethylamine (0.05 mL), and then sealed and left undisturbed for two weeks at RT. The resulting buff block-shaped crystals of **1** were collected in 62% yield, based on zinc content. This complex was unstable in air and insoluble in common organic solvents, such as acetone, methanol, ethanol, dichloromethane, acetonitrile, chloroform, and DMF. FTIR (KBr):  $\tilde{\nu} = 3425$  (m), 2924 (m), 2854 (w), 1643 (s), 1558 (s), 1388 (s), 1296 (w), 1257 (m), 1103 (m), 1065 (w), 980 (m), 879 (w), 841 (m), 717 (m), 663 (w), 555 (w), 509 cm<sup>-1</sup> (w); elemental analysis calcd (%): C 44.02, H 5.12, N 3.09; found: C 43.91, H 5.33, N 3.67.



**X-ray crystallography:** A buff block-shaped crystal of  $[\text{Zn}_7\text{O}_2(\text{pda})_5(\text{H}_2\text{O})_2]$  (**1**) with approximate dimensions of  $0.42 \times 0.42 \times 0.48$  mm was sealed in a glass capillary with a mother liquor and mounted on a Bruker SMART CCD diffractometer for X-ray structural analysis at 293 K. The structure was solved and refined by using full-matrix least-squares on  $F^2$  values (SHELXTL, Sheldrick).<sup>[32]</sup> In this structure, C27, C28, C29, C30, C31, C32, C33, and C34 (C27', C28', C29', C30', C31', C32', C33', and C34') of the PDA ligand are disordered and split up into two atoms. Non-hydrogen atoms (excluding C29 and C33) were refined anisotropically. Hydrogen atoms were fixed at calculated positions and refined by using a riding mode. Further crystallographic details are given in Table 1 and Table S1 (Supporting Information). CCDC-260571 contains the supplementary crystallographic data for this paper. These data can be obtained free of charge from The Cambridge Crystallographic Data Centre via [www.ccdc.cam.ac.uk/data\\_request/cif](http://www.ccdc.cam.ac.uk/data_request/cif).

Table 1. Crystallographic data for **1**.

formula	$\text{C}_{60}\text{H}_{40}\text{O}_{24}\text{Zn}_7$
$M_w$	1602.51
crystal system	tetragonal
space group	$I4cm$
$a$ [Å]	34.6957(5)
$c$ [Å]	41.0328(12)
$V$ [Å <sup>3</sup> ]	49394.9(18)
$Z$	8
$T$ [K]	293
$\lambda$ [Å]	0.71073
$\rho_{\text{calcd}}$ [g cm <sup>-3</sup> ]	0.431
$\mu$ [mm <sup>-1</sup> ]	0.689
$F(000)$	6416
measured data	149079
unique data	28397
observed data [ $I > 2\sigma(I)$ ]	9264
goodness-of-fit on $F^2$	1.069
$R_1^{\text{[a]}}$	0.1100
$wR_2^{\text{[b]}}$	0.2981

$$\text{[a]} R_1 = \sum ||F_o| - |F_c|| / \sum |F_o| \cdot \text{[b]} wR_2 = [\sum w(F_o^2 - F_c^2)^2 / \sum w(F_c^2)^2]^{1/2}.$$

## Acknowledgements

This work was supported by the State Basic Research Project (G2000077507) and the National Nature Science Foundation of China (Grant nos. 29873017, 20273026, and 20101004).

- [1] S. R. Batten, R. Robson, *Angew. Chem.* **1998**, *110*, 1558; *Angew. Chem. Int. Ed.* **1998**, *37*, 1460.
- [2] H. Li, M. Eddaoudi, M. O'Keeffe, O. M. Yaghi, *Nature* **1999**, *402*, 276.
- [3] G. Férey, C. Serre, C. Mellot-Draznieks, F. Millange, S. Surble, J. Dutour, I. Margiolaki, *Angew. Chem.* **2004**, *116*, 6456; *Angew. Chem. Int. Ed.* **2004**, *43*, 6296.
- [4] X. Zhao, B. Xiao, A. J. Fletcher, K. M. Thomas, D. Bradshaw, M. J. Rosseinsky, *Science* **2004**, *306*, 1012.
- [5] B. Moulton, M. J. Zaworotko, *Chem. Rev.* **2001**, *101*, 1629.
- [6] S. Noro, S. Kitagawa, M. Kondo, K. Seki, *Angew. Chem.* **2000**, *112*, 2161; *Angew. Chem. Int. Ed.* **2000**, *39*, 2081.

- [7] P. J. Hagrman, D. Hagrman, J. Zubieta, *Angew. Chem.* **1999**, *111*, 2798; *Angew. Chem. Int. Ed.* **1999**, *38*, 2638.
- [8] J. S. Seo, D. Whang, H. Lee, S. I. Jun, J. Oh, Y. J. Jeon, K. Kim, *Nature* **2000**, *404*, 982.
- [9] O. R. Evans, H. L. Ngo, W. Lin, *J. Am. Chem. Soc.* **2001**, *123*, 10395.
- [10] Q. R. Fang, G. S. Zhu, M. Xue, J. Y. Sun, Y. Wei, S. L. Qiu, R. R. Xu, *Angew. Chem.* **2005**, *117*, 3913; *Angew. Chem. Int. Ed.* **2005**, *44*, 3845.
- [11] R. Xiong, X. You, B. F. Abrahams, Z. Xue, C. Che, *Angew. Chem.* **2001**, *113*, 4554; *Angew. Chem. Int. Ed.* **2001**, *40*, 4422.
- [12] J. P. Zhang, Y. Y. Lin, X. C. Huang, X. M. Chen, *J. Am. Chem. Soc.* **2005**, *127*, 5495.
- [13] J. Y. Sun, L. H. Weng, Y. M. Zhou, J. X. Chen, Z. X. Chen, Z. C. Liu, D. Y. Zhao, *Angew. Chem.* **2002**, *114*, 4651; *Angew. Chem. Int. Ed.* **2002**, *41*, 4471.
- [14] X. Shi, G. S. Zhu, S. L. Qiu, K. L. Huang, J. H. Yu, R. R. Xu, *Angew. Chem.* **2004**, *116*, 6644; *Angew. Chem. Int. Ed.* **2004**, *43*, 6482.
- [15] S. Kitagawa, R. Kitaura, S. Noro, *Angew. Chem.* **2004**, *116*, 2388; *Angew. Chem. Int. Ed.* **2004**, *43*, 2334.
- [16] N. L. Rosi, J. Eckert, M. Eddaoudi, D. T. Vodak, J. Kim, M. O'Keeffe, O. M. Yaghi, *Science* **2003**, *300*, 1127.
- [17] M. Eddaoudi, D. B. Moler, H. Li, B. Chen, T. M. Reineke, M. O'Keeffe, O. M. Yaghi, *Acc. Chem. Res.* **2001**, *34*, 319.
- [18] J. Kim, B. Chen, T. M. Reineke, H. Li, M. Eddaoudi, D. B. Moler, M. O'Keeffe, O. M. Yaghi, *J. Am. Chem. Soc.* **2001**, *123*, 8239.
- [19] Q. R. Fang, X. Shi, G. Wu, G. Tain, G. S. Zhu, R. W. Wang, S. L. Qiu, *J. Solid State Chem.* **2003**, *176*, 1.
- [20] B. Kesanli, Y. Cui, M. R. Smith, E. W. Bittner, B. C. Bockrath, W. B. Lin, *Angew. Chem.* **2005**, *117*, 74; *Angew. Chem. Int. Ed.* **2005**, *44*, 72.
- [21] S. Y. Yang, L. S. Long, R. B. Huang, L. S. Zheng, *Chem. Commun.* **2002**, 472.
- [22] V. Srikant, D. Clarke, *J. Appl. Phys.* **1997**, *81*, 6357.
- [23] Y. Q. Tian, C. X. Cai, Y. Ji, X. Z. You, S. M. Peng, G. H. Lee, *Angew. Chem.* **2002**, *114*, 1442; *Angew. Chem. Int. Ed.* **2002**, *41*, 1384.
- [24] The thermogravimetric analysis (TGA) shows that the weight loss of 30.82% as the temperature increased from 35 to 220°C corresponds to the decomposition of six guest H<sub>2</sub>O, four EtOH, five DMF, and two coordinated H<sub>2</sub>O molecules (calculated: 30.64%). Decomposition of **1** commenced above 320°C.
- [25] M. Eddaoudi, H. L. Li, O. M. Yaghi, *J. Am. Chem. Soc.* **2000**, *122*, 1391.
- [26] P. Wang, A. M. Wang, B. Z. Ding, Z. Q. Hu, *J. Alloys Compd.* **2002**, *334*, 243.
- [27] M. R. Smith, E. W. Bittner, W. Shi, J. K. Johnson, B. C. Bockrath, *J. Phys. Chem. B* **2003**, *107*, 3752.
- [28] Q. L. Zhang, D. J. Wang, J. J. Xu, J. Cao, J. Z. Sun, M. Wang, *Mater. Chem. Phys.* **2003**, *82*, 525.
- [29] V. Duzhko, V. Yu. Timoshenko, F. Koch, T. Dittrich, *Phys. Rev. B* **2001**, *64*, 075204.
- [30] B. O'Regan, M. Grätzel, *Nature* **1991**, *353*, 737.
- [31] T. Dittrich, V. Duzhko, F. Koch, V. Kytin, J. Rappich, *Phys. Rev. B* **2001**, *65*, 155319.
- [32] G. M. Sheldrick, *SHELXTL V5.1 Software Reference Manual*, Bruker AXS, Madison, Wisconsin (USA), **1997**.

Received: August 8, 2005  
Published online: March 3, 2006